Reconstruction of Past Environment and Climate Using Wetland Sediment Records from the Sierra Nevada

Gonzalo Jiménez-Moreno, Antonio García-Alix, R. Scott Anderson, María J. Ramos-Román, Jon Camuera, José Manuel Mesa-Fernández, Jaime L. Toney, Francisco J. Jiménez-Espejo, José S. Carrión, Alejandro López-Avilés, Marta Rodrigo-Gámiz, and Cole E. Webster

Abstract

Understanding the effects of climate change and human activities on fragile mountain ecosystems is necessary to successfully managing these environments under future climate scenarios (e.g., global warming, enhanced aridity). This can be done through the study of paleoecological records, which can provide long paleoenvironmental databases containing information on how ecosystems reacted to climate change and human disturbances before the historical record. These studies can be particularly interesting when focusing on especially warm and/or dry past climatic phases. Biotic (pollen, charcoal) and abiotic (physical, geochemistry) analyses from wetland sediment records from the Sierra Nevada, southern Spain record changes in vegetation, fire history and lake sedimentation since ~11,700 years (cal yr BP). This multiproxy paleoecological study indicates that maxima in temperature and humidity occurred in the area in the Early and Middle Holocene, with a peak in precipitation between ~10,500 and 7000 cal yr BP. This is deduced by maxima in water runoff, the highest abundance of tree species and algae and high total organic carbon values recorded in the alpine wetland's sedimentary records of the Sierra Nevada during that time period. In the last 7000 cal yr BP, and especially after a transition period between ~7000 and 5000 cal yr BP, a progressive aridification process took place, indicated by the decrease in tree species and the increase in xerophytic herbs in this region and a reduction in water runoff evidenced by the decrease in detritic input in the wetland sedimentary records. An increasing trend in Saharan dust deposition in the Sierra Nevada wetlands is also recorded through inorganic geochemical proxies, probably due to a coetaneous loss of vegetation cover in North Africa. The process of progressive aridification during the Middle and Late Holocene was interrupted by millennial-scale climatic oscillations and several periods of relative humid/droughty conditions and warm/cold periods have been identified in different temperature and/or precipitation proxies. Enhanced human impact has been observed in the Sierra Nevada in the last ~3000 cal yr BP through the increase in fires, grazing, cultivation, atmospheric pollution as well as reforestation by *Pinus* and the massive cultivation of *Olea* at lower altitudes.

Keywords

Holocene • Environmental change • Climate change • Human impact • Alpine wetlands • Sierra Nevada • Southern Spain

G. Jiménez-Moreno (✉) · A. García-Alix · A. López-Avilés · M. Rodrigo-Gámiz
Departamento de Estratigrafía y Paleontología, Universidad de Granada, Granada, Spain
e-mail: gonzaloj@ugr.es

A. García-Alix · J. M. Mesa-Fernández · F. J. Jiménez-Espejo
Instituto Andaluz de Ciencias de la Tierra (IACT), CSIC-UGR, Armilla, Spain

R. S. Anderson · C. E. Webster
School of Earth and Sustainability, Northern Arizona University, Flagstaff, USA

M. J. Ramos-Román · J. Camuera
Department of Geosciences and Geography, University of Helsinki, Helsinki, Finland

J. L. Toney
School of Geographical and Earth Sciences, University of Glasgow, Glasgow, UK

J. S. Carrión
Department of Plant Biology, Faculty of Biology, University of Murcia, Murcia, Spain

1 Introduction

Alpine environments are especially fragile and sensitive to recent climate change, which is causing altitudinal displacements of plant and animal species, and loss of

R. Zamora and M. Oliva (eds.), *The Landscape of the Sierra Nevada*,
https://doi.org/10.1007/978-3-030-94219-9_7

biodiversity (Thuiller et al. 2005; Gehrig-Fasel et al. 2008; Malanson et al. 2019). The stress on the biotic component of ecosystems is intensified when adding the effect of recent and projected drought in the Mediterranean region (Páscoa et al. 2017; Sousa et al. 2019), which will also cause enhanced fire activity (Pausas and Fernández-Muñoz 2012; IPCC 2013; Sousa et al. 2015).

The study of past environment and climate changes is necessary to improve our insight on future climate scenarios by providing information on how mountain ecosystems responded to long- and short-term variations in climate during the Holocene (last 11,700 years), particularly during warmer and drier climates. In this respect, wetlands in the Sierra Nevada are a model system for such studies, as they are remote and relatively pristine areas of high biodiversity, not significantly modified by human activities and preserve a high-quality signal of past Holocene natural and anthropogenic environmental and climate change (see references below).

The footprint of climate change and human impact and the generated response in the environment (e.g., changes in vegetation, fires, erosion, pollution) is recorded in lake sediments, for example, through the accumulation of fossil remains, charcoal fragments, presence of specific biomarkers, sediment granulometry and elemental chemical composition. In this respect, a significant effort has been made in the last decade by our research group to further multidisciplinary study of sediment records from seven alpine lakes and bogs in the Sierra Nevada to understand paleoenvironmental and paleoclimate change (Anderson et al. 2011; Jiménez-Moreno and Anderson 2012; García-Alix et al. 2012, 2013, 2017, 2018, 2020; Jiménez-Espejo et al. 2014; Jiménez-Moreno et al. 2013, 2020; Ramos-Román et al. 2016, 2018a, b, 2019, 2021; Mesa-Fernández et al. 2018; Camuera et al. 2018, 2019; Manzano et al. 2019; Toney et al. 2020). Here we provide a review of the research in alpine wetland sedimentary records from the Sierra Nevada with the main goal of linking biotic changes with climate and human impacts on these fragile environments.

2 Materials and Methods

2.1 Sierra Nevada Sites

In this study, we used multi-proxy (lithological, sedimentological, palynological, anthracological, geochemical) data from seven radiometrically well-dated Holocene sedimentary records from wetland sites located at different elevation and orientations in the Sierra Nevada area (Fig. 1; Table 1). These sedimentary lake and bog archives were recovered by the authors between 2006 and 2015 (Table 1). Six of the studied sites are situated above treeline in the cryoromediterranean vegetation belt where typical vegetation is alpine tundra, while one site occurs in the mesomediterranean vegetation belt, where natural potential vegetation is mostly characterized by evergreen sclerophyllous oak forests. Three sites—Laguna de la Mula (LdlM) (Jiménez-Moreno et al. 2013), Laguna de la Mosca (LdlMo) (Manzano et al. 2019) and Borreguil de la Virgen (BdlV) (García-Alix et al. 2012; Jiménez-Moreno and Anderson, 2012)—are situated at the north-facing side of the Sierra Nevada, while three others—Laguna de Río Seco (LdRS) (Anderson et al. 2011; García-Alix et al. 2013, 2018; Jiménez-Espejo et al. 2014; Toney et al. 2020), Borreguil de la Caldera (BdlC) (Ramos-Román et al. 2016; García-Alix et al. 2017) and Laguna Hondera (LH) (Mesa-Fernández et al. 2018)—are located in the south face. The Padul wetland site is located at the southwest foothills of the Sierra Nevada (Camuera et al. 2018, 2019, 2021; Ramos-Román et al. 2018a, b; Webster 2018). These sites are thus situated between ~725 m in the mesomediterranean to ~3020 m in the cryoromediterranean vegetation belt (Table 1).

2.2 Sedimentary Records: Sediment Collection, Chronology, Lithology and Magnetic Susceptibility

Sediment core collection in the alpine Sierra Nevada sites was done using a Livingstone square-rod piston corer in the visual depocenter of the studied wetlands. Coring in lakes was done from a floating platform anchored to shore and short cores with the unconsolidated 10–20 cm of the lake sediment records were retrieved using a universal corer (Aquatic Research Inc). Padul-15–05 core was collected using a Rolatec RL-48-L drilling machine equipped with a hydraulic piston corer from the Scientific Instrumentation Centre of the University of Granada (CIC-UGR). The sediment cores were wrapped in plastic wrap and alu minum foil in the field, put in core boxes, and transported back to the laboratory where they were stored in a cool room at 4 °C.

The chronology for the different wetland sedimentary records was constrained using accelerator mass spectrometry (AMS) radiocarbon dates from plant remains and organic bulk samples taken from the cores. ICP-MS Plutonium, ^{210}Pb and ^{137}Cs profiles were also built on the uppermost part of the lake sedimentary cores (Table 1). Radiocarbon dates were calibrated with the IntCal13.14C calibration curve (Reimer et al. 2013), and used together with the Pb, Cs and Pu dates and the year of core sampling as the top of the sediment record in order to build accurate and robust age-depth models (Fig. 2). Age models for the individual sites were built using different approaches, including linear interpolation (BldV, LdlMo) and smooth spline option

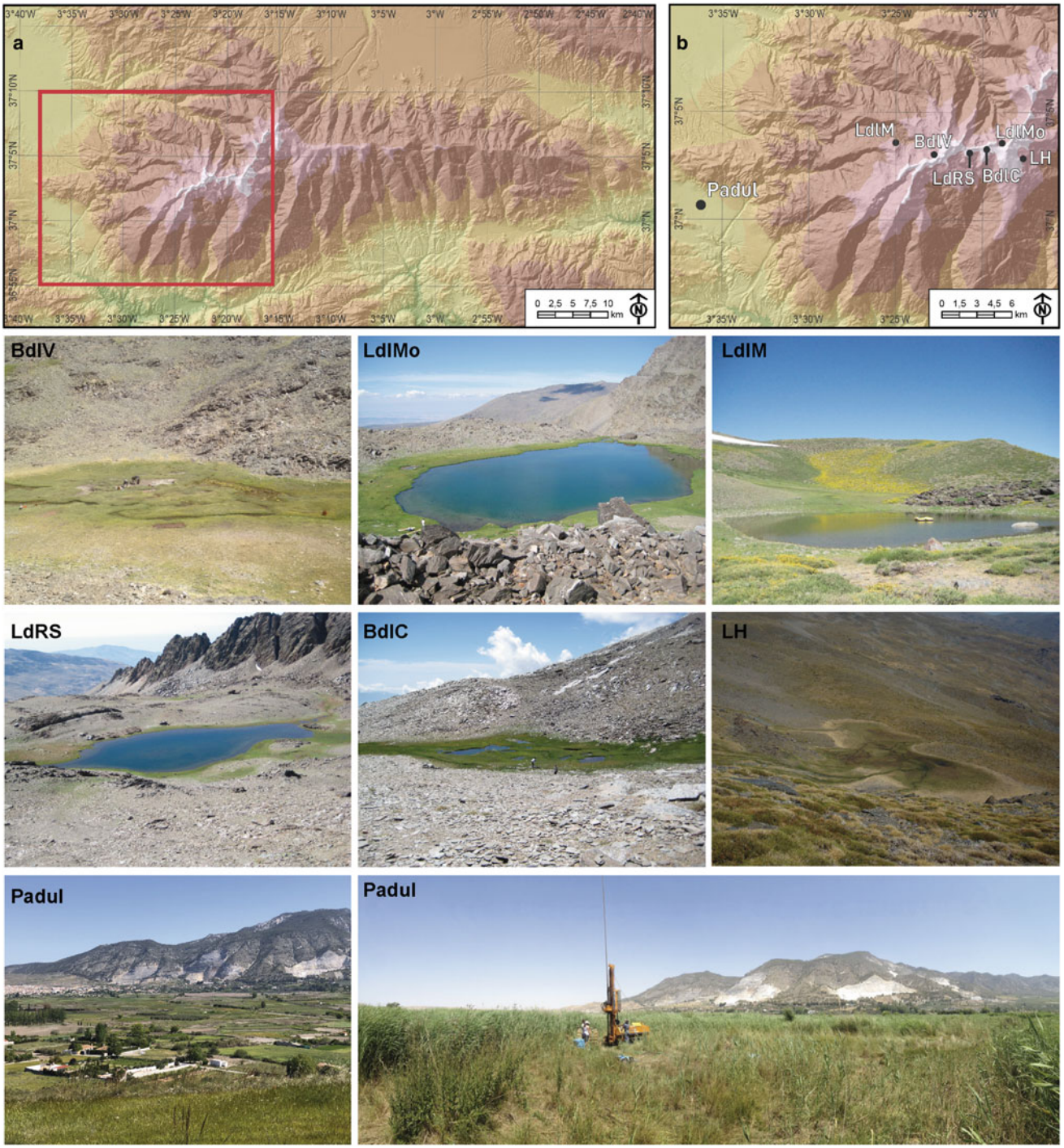

Fig. 1 Sierra Nevada wetland site location and photographs. **a** Map of the Sierra Nevada mountain range, southern Iberian Peninsula. The rectangle shows the magnified area shown in **b**. **b** Site location of the Sierra Nevada mutiproxy records used in this study: Laguna de Río Seco (LdRS), Borreguil de la Caldera (BdlC), Borreguil de la Virgen (BdlV); Laguna de la Mosca (LdlMo), Laguna Hondera (LH), Laguna de la Mula (LdlM), and Padul-15–05 (Padul). See Table 1 and text for explanation

(LdRS, BdlC, LH, LdlM, Padul) using the "clam" software (Blaauw 2010; Fig. 2) or Heegaard et al. (2005) approach to calculate the age-depth (see original studies for more details on the age model construction; Table 1).

The lithology of the Sierra Nevada sediment cores (Fig. 2) was described from split core segments in the laboratory (Table 1). Magnetic susceptibility (MS), a measure of the tendency of sediment to carry a magnetic charge

Table 1 Site description of the Sierra Nevada records synthetized in this study. Sites from the Sierra Nevada are: BdlV: Borreguil de la Virgen; LdlMo: Laguna de la Mosca; LdlM: Laguna de la Mula; LdRS: Laguna de Río Seco; BdlC: Borreguil de la Caldera; LH: Laguna Hondera; Padul: Padul peat bog. Asterisks (*) indicate information for the Holocene part of those sedimentary records

Site	Coordinates and altitude (m asl)	Vegetation belt	Site environment	Core length (cm)	Period covered (cal yr BP)	Dating method	References
BdlV	37°03′15″N, 3°22′40″ W; 2945 m	Cryoromediterranean	Peatland	169	0–8200	9 AMS ^{14}C dates	Jiménez-Moreno and Anderson (2012), García-Alix et al. (2012)
LdlMo	37°03′ 34.88″N, 3° 18′52.98″W; 2889 m	Cryoromediterranean	Lake	190	0–8300	10 AMS ^{14}C dates, 1 Pu profile	Manzano et al. (2019)
LdlM	37°3.583′N, 3°25.017′W; 2497 m	Cryoromediterranean	Lake	32.5	0–4100	6 AMS ^{14}C dates	Jiménez-Moreno et al. (2013)
LdRS	37°02.43″N, 3°20.57′W; 3020 m	Cryoromediterranean	Lake	150	0–11,000	9 AMS ^{14}C dates, 1 ^{137}Cs, 1 ^{210}Pb profiles	Anderson et al. (2011), García-Alix et al. (2013, 2020), Jiménez-Espejo et al. (2014), Toney et al. (2020)
BdlC	37°03′02″ N, 3°19′24″ W; 2992 m	Cryoromediterranean	Peatland	56	0–4400	5 AMS ^{14}C dates	Ramos-Román et al. (2016), García-Alix et al. (2017)
LH	37°02.88′N, 3°17.66′W; 2899 m	Cryoromediterranean	Lake	83	0–11,000	7 AMS ^{14}C dates	Mesa-Fernández et al. (2018)
Padul	37°00′ 39.77″N, 3° 36′14.06″W; 725 m	Mesomediterranean	Lake/Peatland	327*	0–11,000	14 AMS ^{14}C dates*	Ramos-Román et al. (2018a, b), Camuera et al. (2018, 2019)

(Snowball and Sandgren 2001), was measured with a Bartington MS2E meter in dimensionless SI units (Fig. 2). Measurements were taken directly from the core surface every 0.5 cm for the entire length of the cores.

2.3 Inorganic Geochemistry

Inorganic geochemical analyses in sediment samples from cores LdRS and LH were performed by means of (1) inductively coupled plasma mass spectrometry (ICP-MS for minor and trace elements in both cores), (2) flame Atomic Absorption (AAS for major elements in LdRS core) and (3) inductively coupled plasma–optical emission spectrometry (ICP-OES for major elements in LH core) (Table 1) at the Centro de Instrumentación Científica of the University of Granada (CIC-UGR). See details in Jiménez-Espejo et al. (2014) and Mesa-Fernández et al. (2018).

Additionally, high-resolution and continuous elemental geochemical analyses from the BdlC, LH and Padul Sierra Nevada cores were obtained using an Avaatech X-Ray fluorescence (XRF) core Scanner at the XRF-Core Scanner Laboratory (University of Barcelona, Spain). The cores were scanned two times with a point sensor: one at 10 s count time (10 kV X-ray voltage and 650 mA X-ray current for light elements), and another one at 35 s count time (30 kV X-ray voltage and 1700 mA X-ray current for heavy elements). See details in García-Alix et al. (2017), Mesa-Fernández et al. (2018), Camuera et al. (2019).

2.4 Organic Geochemistry—Bulk Sediments and Specific Organic Lipids

The elemental composition (C and N) of bulk sediment samples was measured (after acid digestion to remove potential carbonates) using a Thermo Scientific Flash 2000 elemental analyzer at CIC-UGR. C isotopes were measured in an aliquot of the same samples by means of isotope-ratio mass spectrometry (IRMS) with a coupled elemental analyzer (EA). We used two different configurations: a Carlo Erba Ba 1500 series 2 EA attached to a Thermo Finnigan Delta plus XL IRMS (Instituto Andaluz de Ciencias de la Tierra CSIC-UGR, Spain) in samples from LdlM, BdlV and

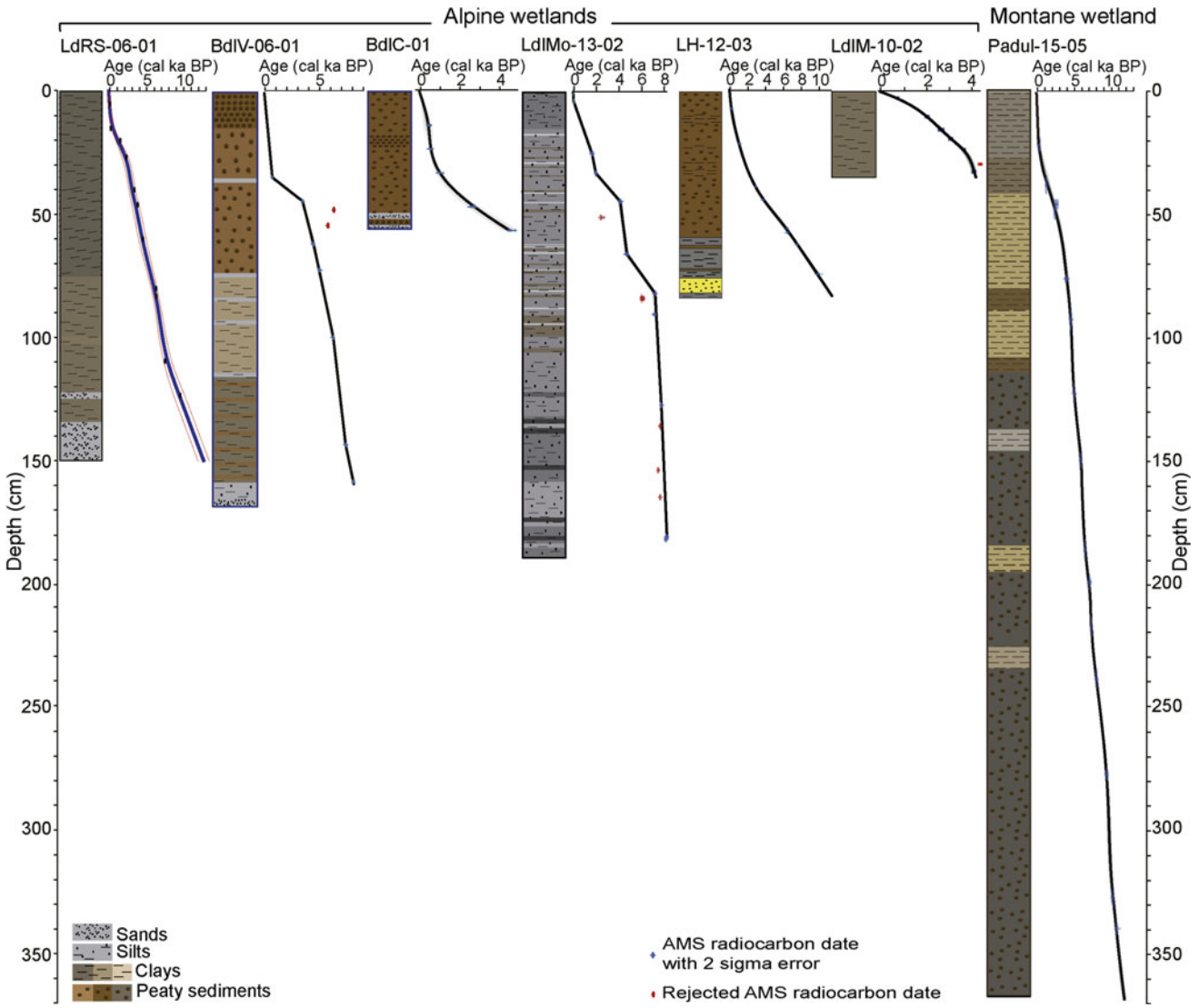

Fig. 2 Sediment core lithology and age–depth models for the studied Sierra Nevada records. Red squares are radiocarbon dates that were not used in the age models. The studied sites are Laguna de Río Seco (LdRS-06–01: LdRS), Borreguil de la Caldera (BdlC-01: BdlC), Borreguil de la Virgen (BdlV-06–01: BldV); Laguna de la Mosca (LdlMo-10–02: LdlMo), Laguna Hondera (LH-12–03: LH), Laguna de la Mula (LdlM-10–02: LdlM), and Padul (Padul-15–05: Padul)

LdRS, and a Euro EA 300 EA attached to an Isoprime 50 V IRMS (CIC-UGR) in samples from BdlC. The isotopic measurements were calibrated using internal and international standards, and expressed using the δ notation and the reference V-PDB. See details in García-Alix et al. (2012, 2017), Jiménez Moreno et al. (2013), Jiménez-Espejo et al. (2014), Camuera et al. (2019).

Lipid extractions were performed by means of silica gel chromatography using different solvents in order to separate the organic compounds depending on their polarity. The *n*-alkanes were analyzed at the BECS laboratory (University of Glasgow, UK) by means of a Shimadzu 2010 GC-FID in order to quantify them. Long chain diols were analyzed after derivatization by bis- (trimethylsilyl) trifluoroacetamide (BSTFA) at the BECS laboratory (University of Glasgow, UK) in the Shimadzu QP2010 Plus mass spectrometer interfaced with a Shimadzu 2010 GC using a scan mode. Afterwards, an ion monitoring mode (SIM) was selected specifying the characteristic fragment ions of the most important long-chain diols (C_{28}, C_{30} and C_{32} diols). See more details in Garcia-Alix et al. (2020) and Toney et al. (2020).

2.5 Palynological Analysis

Sample processing for pollen analysis in all the alpine Sierra Nevada records was done following a modified Faegri and Iversen (1989) methodology, using 1 cm^3 of sediment.

Processing included treatment with sodium hexametaphosphate for clay deflocculation, addition of *Lycopodium* spores for calculation of pollen concentration, sieving, HCl, HF and acetolysis solution. Pollen residue was suspended in silicone oil (for the LdRS record) and glycerol (for the rest of the studied records), and analyzed at 400 magnifications using a light microscope with a goal of the identification of 300 terrestrial pollen grains. Pollen identification was done with the help of modern pollen collections at the University of Granada, University of Murcia and Northern Arizona University and modern pollen atlases (for example, Reille 1992; Beug 2004). Raw pollen counts were transformed to pollen percentages based on the terrestrial pollen sum. Arboreal pollen (AP) was calculated with the sum of tree pollen divided by the total terrestrial (tree, herbs and shrubs) pollen.

2.6 Charcoal

Samples for macroscopic charcoal analysis (1 cm^3) were taken every 0.5 cm throughout selected Sierra Nevada sediment cores (LdRS, LdlMo, LdlM and BdlC). Charcoal analysis followed the protocol described in Whitlock and Anderson (2003). Processing included pretreatment with sodium hexametaphosphate to deflocculate clays and sieving with mesh sizes of 250 and 125 µm. Counting of charcoal particles was performed with a stereomicroscope at 10–70 magnifications. Charcoal counts for each sample were converted to charcoal concentrations [CHAC; number of charcoal particles per cm^3 or cubic centimeter (cc)].

3 Results

3.1 Age Control of the Sedimentary Sequences

The age-depth models for the studied Sierra Nevada records are constrained by a total of 60 AMS ^{14}C radiocarbon dates and 3 ICP-MS Plutonium, ^{210}Pb and ^{137}Cs profiles for the upper part of the LdRS and LdlMo records (Fig. 2; Table 1). All the absolute age data fall within the Holocene period (11,700–0 cal yr BP). The age of wetland formation and beginning of sediment accumulation in the studied basins shows a three-step chronological pattern at slightly older than ~11,000, ~8200 and ~4200 cal yr BP.

3.2 Lithology and Magnetic Susceptibility (MS)

Sediment coring in all the studied sites from alpine Sierra Nevada ended when coarse sediments were reached and the human-powered Livingstone corer was unable to deepen any further. Therefore, many of those cores are relatively inorganic in the lowermost portion of the cores, progressively becoming more organic higher in the sedimentary sequence (Fig. 2). Overall, the lithology of the lake records is mostly characterized by clays and silts, whereas lithology in the locally called "borreguiles" (peat bogs) cores is dominated by peat. Very organic-rich clay (called gyttja) sediments characterize most of the LdRS and LdlM sediment cores. The 190-cm-long LdlMo is the longest of all the alpine Sierra Nevada sediment records and it is dominated by silty clays, which vary greatly in grain size and color. A similar lithological sedimentary sequence is observed in the BdlV and LH cores, with high sand content at the core bottom, overlain by clays and transitioning into peats in the Middle Holocene, which dominate until Present (Jiménez-Moreno and Anderson 2012; Mesa-Fernández et al. 2018; Fig. 2). The Late Holocene BdlC core, also located in a peat bog, is shorter and shows sand at the bottom and then peat for the rest of the record. Lithology of the Padul record is characterized by dark organic rich peat sediments from ~11,600 to ~7600 cal yr BP. Dark organic-rich peats with intercalations of three grey or brown clay layers occurred between ~7600 and 4700 cal yr BP. The uppermost 4700 cal yr BP of the record are characterized by clays and clayey-carbonates (Ramos-Román et al. 2018a, b).

Holocene MS records from the Sierra Nevada show unique individual patterns but share long- and short-scale variations (Fig. 3). The Early Holocene in the alpine Sierra Nevada environments (i.e., LdRS and LH records) is characterized by overall high MS values. This contrasts with very low MS values recorded during the Early Holocene in the lower elevation sedimentary record from Padul. MS values decreased during the Middle Holocene reaching minima in some of the records right at the transition with the Late Holocene (between ~5000 and 4400 cal yr BP). MS depicts an increasing trend in the Late Holocene (clear in Padul, LH, LdlMo and LdlM).

3.3 Inorganic Geochemistry

In order to simplify, in this section we show a synthesis of the most environmentally significant variations in major and trace element concentrations from the studied Sierra Nevada sites (Fig. 4; check specific publications for more detailed information). The Early Holocene and early-Middle Holocene (from ~11,000 until ~7000 cal yr BP) in LH is characterized by maximum values of K/Ti ratios, coinciding with the lowest values in Ca/Al, Ca/Ti and Zr/Al ratios (Mesa-Fernández et al. 2018). On the other hand, an opposite pattern is observed in Zr/Th data from LdRS, LH and BdlC, which show minima at that time and an increasing trend in the last ~7000 cal yr BP (Jiménez-Espejo et al.

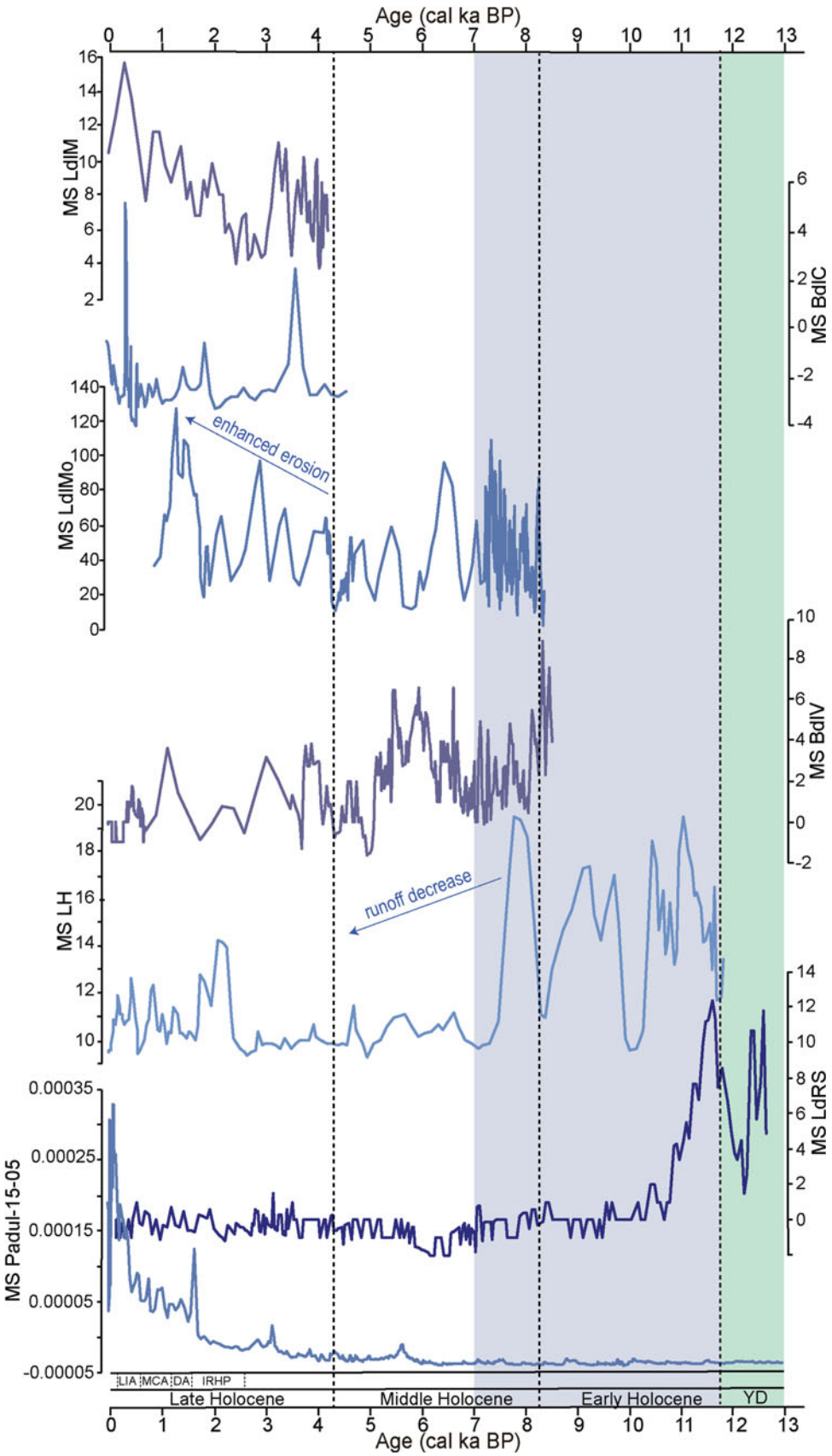

Fig. 3 Magnetic susceptibility (MS) records from the Sierra Nevada sediment cores for the last 13,000 cal yr BP. MS data is shown in SI units. YD stands for Younger Dryas (in green shading color). In grey shading is the warmest-wettest period deduced by other climatic proxies discussed in the text and overall highest MS data. IRHP, DA, MCA and LIA stand for Iberian Roman Humid Period, Dark Ages, Medieval Climate Anomaly and Little Ice Age, respectively

2014; Mesa-Fernández et al. 2018; García-Alix et al. 2017). Pb/Al data from LdRS and LH show low values during most of the Holocene and increase in the Late Holocene, peaking around 3000–2500, 2000 cal yr BP and between 1950–1970 AD (García-Alix et al. 2013; Mesa-Fernández et al. 2018).

3.4 Organic Geochemistry

C/N values are relatively low in the Early and Middle Holocene, oscillating around 10 and 16, recorded in LdRS and BdlV, respectively (Fig. 5). A significant increase occurred at ~6000 cal yr BP in LdRS and at ~5000 cal yr BP in BdlV and maxima are reached until 4000 cal yr BP. A general decreasing trend is observed in all the records (including the BdlC and LdlM records) during the Late Holocene. In the last centuries, the BdlC and BdlV records show a rapid and significant increase. A significant decrease in C/N in the last decades can be observed in all the studied records except for BdlV.

TOC content from LdRS shows very low values (2.1%) between ~11,100 and 10,500 cal yr BP. TOC values increased later on and showed a maximum (11.2%) between ~10,500 and 5700 cal yr BP. TOC values decreased then until present (down to 4.8%).

Values of ™^{13}C from BdlV range from −28.1 to −23.1% with a mean value of −26.4 ± 1.0 ‰ (V-PDB) (Fig. 5). The highest values of ™^{13}C occur from 8200 to 5100 cal yr BP. This record shows a decreasing trend since the early-Middle Holocene, interrupted by several oscillations, until the last 300 years when a significant increase is observed (Fig. 5).

The range of nC$_{21-25}$-alkanes is related to submerged and floating aquatic plants (P$_{aq}$). The Paq values from LdRS range from 0.25 to 0.48 with an average value of 0.37. High Paq values are registered during the Early Holocene between ~11,800 and 10,500 cal yr BP. An increasing trend until ~6300 cal yr BP up to 0.47 values is observed, subsequently to a minimum value of 0.34 around 9300 cal yr BP. Paq decreased linearly after ~6300 cal yr BP and until ~260 cal yr BP, reaching values of 0.29. A fast increase in Paq is detected in the last ~160 years of the record, getting to values of 0.47 (Fig. 5).

The fractional abundance of C$_{28}$ and C$_{30}$ 1,13 and 1,15-diols is expressed in the Long chain Diol Index (LDI) in the LdRS record. LDI values during the Holocene oscillate between 0.05 to 0.31 with a mean value of 0.18 ± 0.5 (Fig. 5). LDI data are higher from ~5000 to 4200 cal yr BP, ~2540, ~1020, and after −10 cal yr BP. LDI values decreased at ~6560, ~6170, between ~4100 and 3900 cal yr BP and significantly between ~450 and 150 cal yr BP and between ~40 and 30 cal yr BP. Highest LDI values are reached at around 4800–4650 cal yr BP and at present.

3.5 Palynological Analysis

Pollen records from the Sierra Nevada show highest AP abundances during the Early and early-Middle Holocene between ~11,500–7000 cal yr BP (LdRS, BdlV and LdlMo at high elevations and Padul-15–05 at lower elevation; Fig. 6). In the alpine environments, the highest abundance of tree species is reached at that time, especially in *Pinus* (most likely *P. sylvestris* or *P. nigra*) and *Quercus* (deciduous), but also in *Betula*, *Alnus* and *Salix* (Anderson et al. 2011; Jiménez-Moreno and Anderson 2012; Manzano et al. 2019). On the other hand, *Artemisia*, *Juniperus* and Amaranthaceae show their minima. Pelagic algae, such as *Botryococcus* and *Pediastrum*, reach maxima during this period (Anderson et al. 2011; Jiménez-Moreno and Anderson 2012). At lower elevation, the Padul record shows high AP (mostly Mediterranean forest with evergreen and deciduous *Quercus*) from ~11,600 to 7600 cal yr BP (Ramos-Román et al. 2018a, b).

The Sierra Nevada pollen records show that between ~7000 and 5000 cal yr BP AP (mostly *Pinus*) remains abundant, but starts showing a decreasing trend (Fig. 6), together with other forest species such as deciduous *Quercus* and *Betula* (Anderson et al. 2011; Jiménez-Moreno and Anderson 2012; Mesa-Fernández et al. 2018; Manzano et al. 2019). Aquatic species also declined considerably at that time (see previous references). A more pronounced decline in forest species is observed in all the Sierra Nevada records from 5000 cal yr BP until the last centuries (Fig. 6). *Pinus* and other forest species (such as *Quercus*) decreased considerably while *Artemisia*, Amaranthaceae or Caryophyllaceae increased (Anderson et al. 2011; Jiménez-Moreno and Anderson 2012; Ramos-Román et al. 2016, 2018b; Mesa-Fernández et al. 2018; Manzano et al. 2019).

The high-elevation (alpine) Sierra Nevada records also show that *Olea* expanded rapidly in the last ~950 cal yr BP (Ramos-Román et al. 2019) and *Pinus* increased in the last centuries (Anderson et al. 2011; Jiménez-Moreno and Anderson 2012; Mesa-Fernández et al. 2018; Manzano et al. 2019) and particularly in the last decades (Ramos-Román et al. 2016). *Sporormiella*, a fungus spore type indicating herbivory, increased considerably in the Late Holocene in LdRS (last 3000 years) and BdlV and BdlC (last 200 years) records (Anderson et al. 2011; Jiménez-Moreno and Anderson 2012; Ramos-Román et al. 2016). Increases in Cerealia pollen, together with other nitrophilous and ruderal

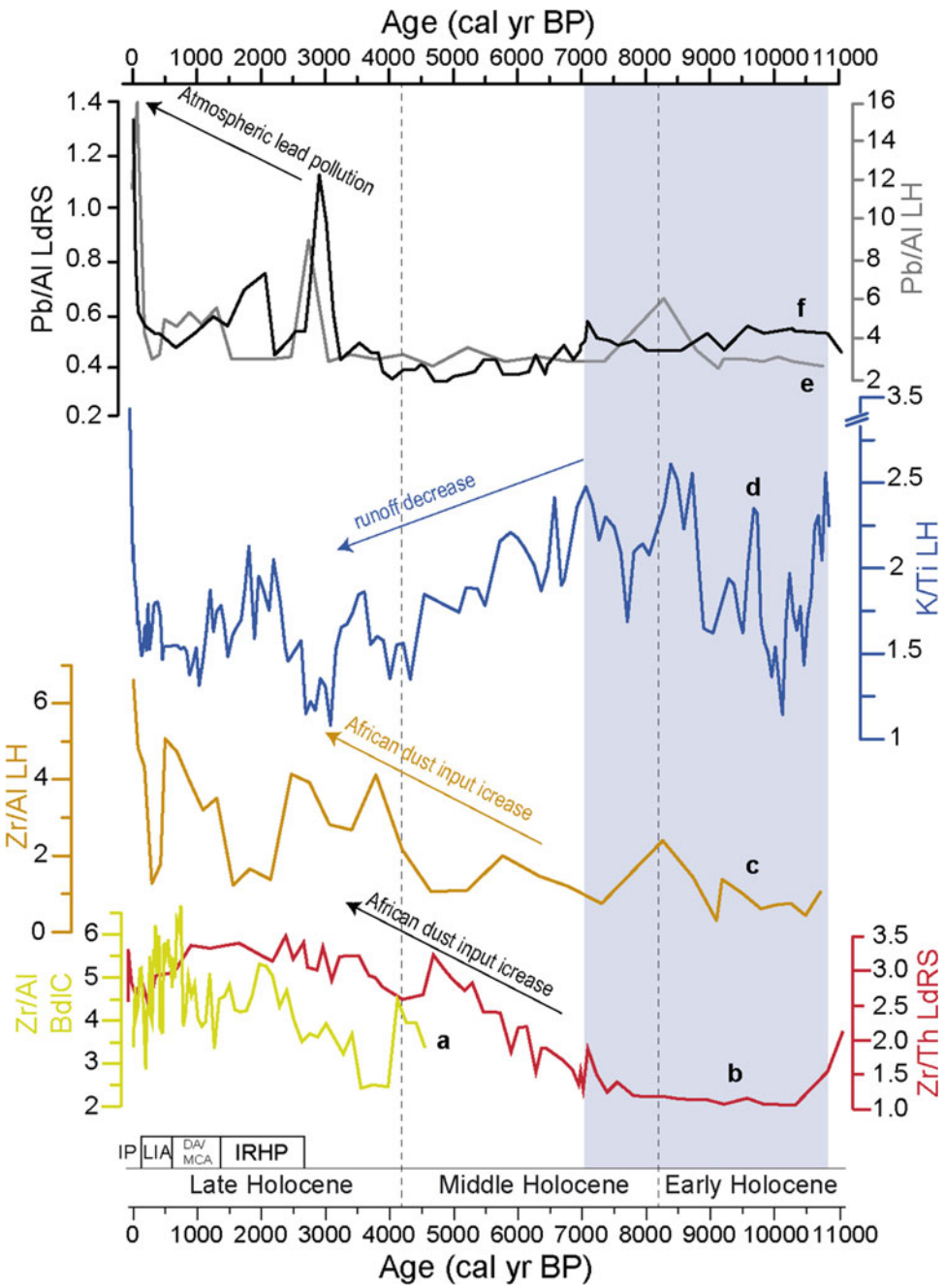

Fig. 4 Inorganic geochemistry data from the studied Sierra Nevada wetland sediment records for the last 11,000 cal yr BP. Runoff, lake level and eolian dust proxies. **a** Zr/Al from Borreguil de la Caldera (BdlC; García-Alix et al. 2017). **b** Zr/Th from Laguna de Río Seco (LdRS) (Jiménez-Espejo et al. 2014). **c** Zr/Al from Laguna Hondera (LH) (Mesa-Fernández et al. 2018). **d** K/Ti from Laguna Hondera (LH; Mesa-Fernández et al. 2018). **e** Pb/Al from Laguna Hondera (LH; Mesa-Fernández et al. 2018). **f** Pb/Al from Laguna de Río Seco (LdRS; García-Alix et al. 2013). IRHP, DA, MCA, LIA and IP stand for Iberian Roman Humid Period, Dark Ages, Medieval Climate Anomaly, Little Ice Age and Industrial Period, respectively. In grey shading is the wettest period deduced by these and other climatic proxies discussed in the text

pollen taxa such as *Rumex*, *Plantago*, Urticaceae or Convolvulaceae are observed in the last ~3000 cal yr BP and are particularly abundant in the last ~1500 cal yr BP.

In addition to the general decreasing trend in tree species after ~7000 cal yr BP, important cyclical variations in pollen abundances are observed, especially in *Pinus* and *Quercus* and thus in AP (Fig. 6). In most of the Sierra Nevada pollen sequences, the AP minima are observed at ~7500, 6500, 5000 and 4200, 3000 and 1200 cal yr BP.

3.6 Charcoal

The occurrence of charcoal particles in the alpine Sierra Nevada Holocene sedimentary records is low, with values ranging between 0 and 20 particles per cubic centimeter (cc) and a maximum value of 60 particles per cc reached in LdRS record (Anderson et al. 2011; Fig. 7). Only one charcoal record, LdRS, is available for the Early Holocene, which suggests relatively low fire occurrence. The Middle Holocene is characterized in the LdRS record by an increase

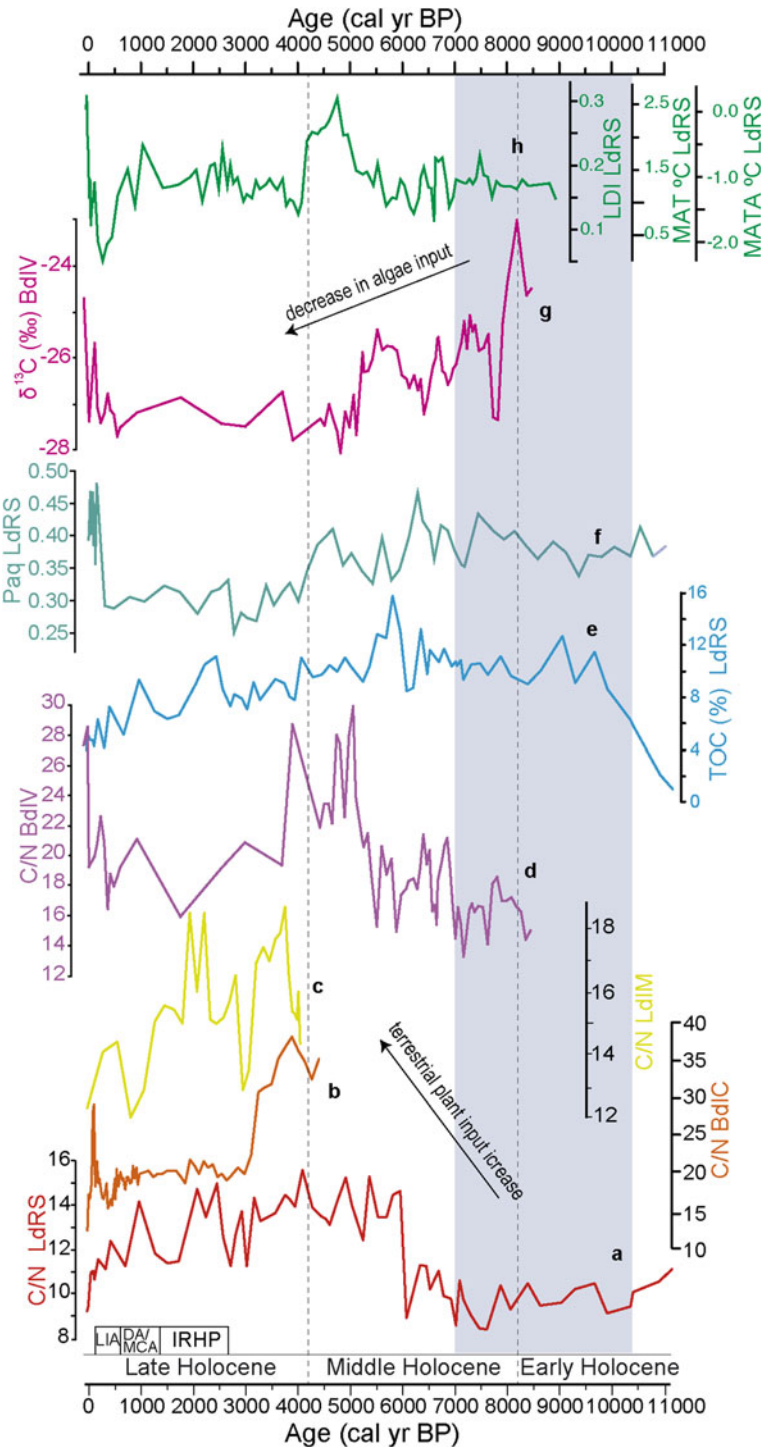

Fig. 5 Organic geochemistry data from the studied Sierra Nevada wetland sediment records for the last 11,000 cal yr BP. **a** C/N from Laguna de Río Seco (LdRS) (Jiménez-Espejo et al. 2014). **b** C/N ratios from Borreguil de la Caldera (BdlC; Ramos-Román et al. 2016). **c** C/N from Laguna de la Mula (LdlM; Jiménez-Moreno et al. 2013). **d** C/N from Borreguil de la Virgen (BdlV; Jiménez-Moreno and Anderson, 2012). **e** Total organic carbon (TOC) content from Laguna de Río Seco (LdRS; Jiménez-Espejo et al. 2014). **f** P_{aq} from Laguna de Río Seco (LdRS; Toney et al. 2020). **g** ™^{13}C from Borreguil de la Virgen (BdlV; García-Alix et al. 2012). **h** LDI record and temperature reconstruction from Laguna de Río Seco (LdRS; García-Alix et al. 2020; Toney et al. 2020). IRHP, DA, MCA and LIA stand for Iberian Roman Humid Period, Dark Ages, Medieval Climate Anomaly and Little Ice Age, respectively. In grey shading is the wettest period deduced by these and other climatic proxies discussed in the text

in charcoal particles, reaching a peak at ~6700 cal yr BP and a secondary lower peak at ~5500 cal yr BP. High relative values are reached in the LdlMo record during the Middle Holocene, with peaks around 7500, 6700 and 5500 cal yr BP. The Late Holocene is characterized in LdRS by an increase in fire activity between 3000 cal yr BP and present and a significant peak between ~2700 and 1600 cal yr BP in LdlM and BdlC records (Fig. 7).

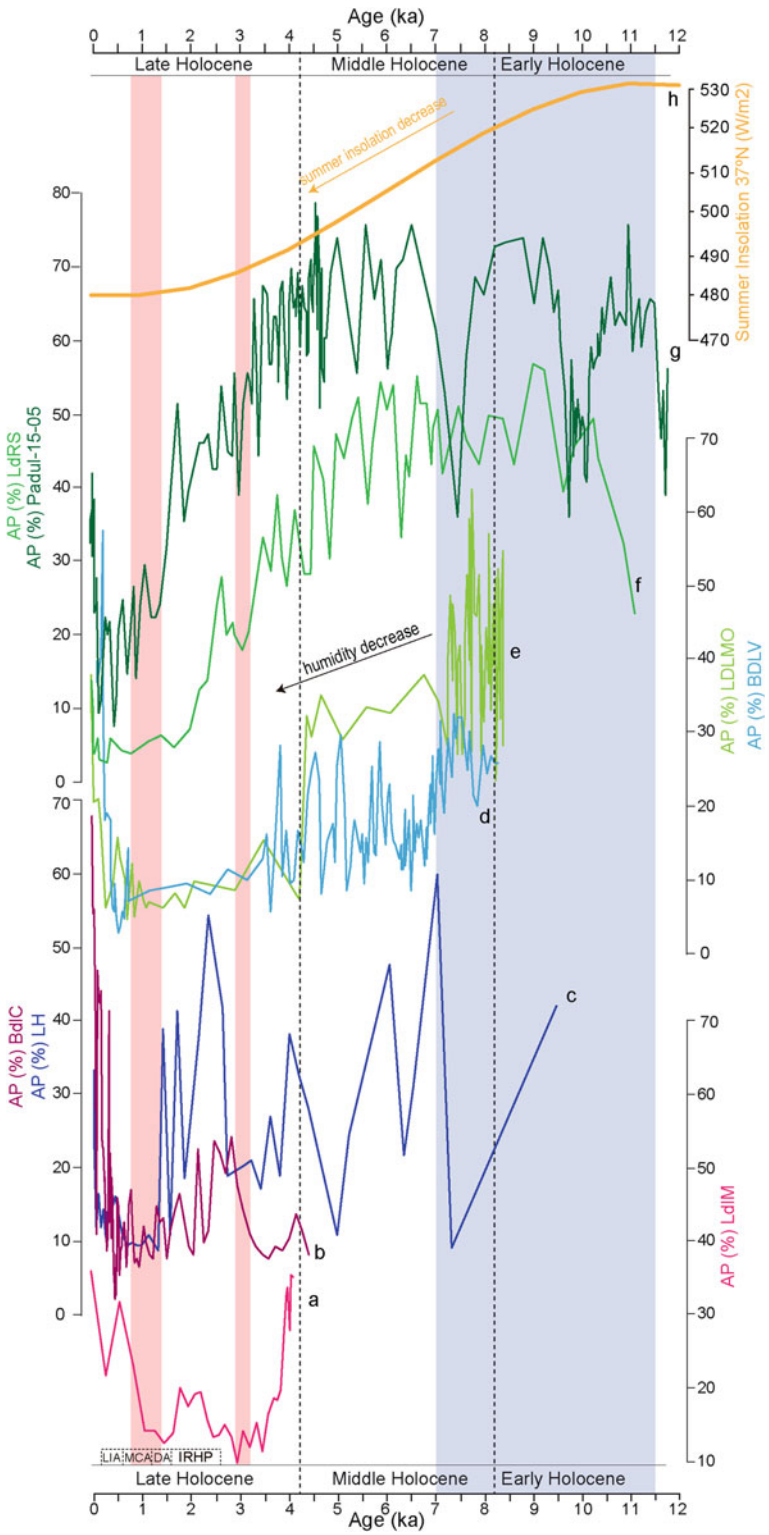

Fig. 6 Arboreal pollen (AP) records from the studied Sierra Nevada wetland sediment cores and summer insolation for the last 12,000 cal yr BP. **a** AP from Laguna de la Mula (LdlM; Jiménez-Moreno et al. 2013). **b** AP from Borreguil de la Caldera (BdlC; Ramos-Román et al. 2016). **c** AP from Laguna Hondera (LH; Mesa-Fernández et al. 2018). **d** AP from Borreguil de la Virgen (BdlV; Jiménez-Moreno and Anderson, 2012). **e** AP from Laguna de la Mosca (Manzano et al. 2019). **f** AP from Laguna de Río Seco (LdRS; Anderson et al. 2011). **g** AP from Padul (Padul-15–05; Ramos-Román et al. 2018a, b). **h** Summer insolation for 37 °N (Laskar et al. 2004). IRHP, DA, MCA and LIA stand for Iberian Roman Humid Period, Dark Ages, Medieval Climate Anomaly and Little Ice Age, respectively. In grey shading is the deduced warmest and wettest period. In red shading are especially arid periods of the Late Holocene that triggered forest reductions

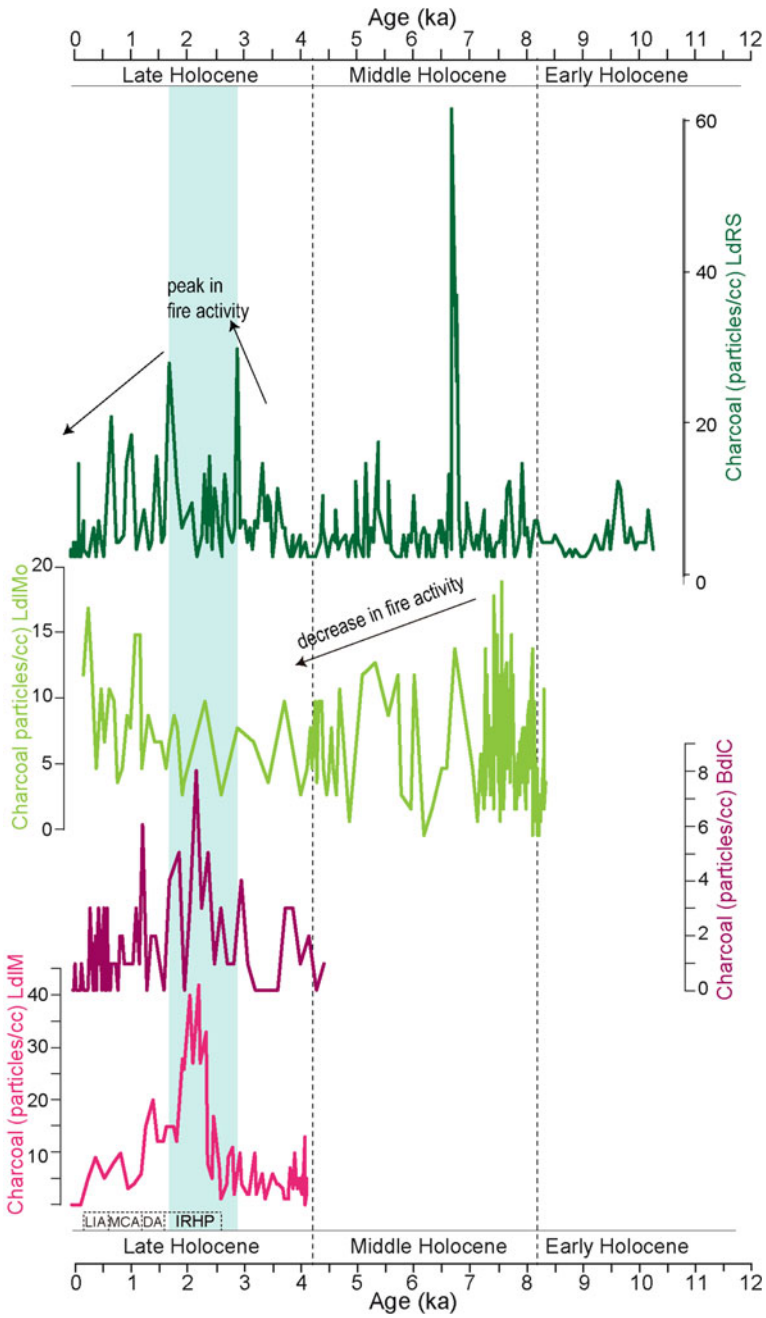

Fig. 7 Charcoal records from the studied Sierra Nevada wetland sediment cores indicate fire activity for the last 12,000 cal yr BP. IRHP, DA, MCA and LIA stand for Iberian Roman Humid Period, Dark Ages, Medieval Climate Anomaly and Little Ice Age, respectively. The blue shading highlights an overall increase in charcoal and thus fire activity coinciding with the IRHP

4 Discussion

4.1 Age of the Sedimentary Sequences

Geomorphologic evidences show that alpine environments above 2000–2200 m in the north face and 2300–2400 m in the south face in the Sierra Nevada were glaciated during the Last Glacial Cycle and valley and cirque glaciers occupied and eroded the basins where the lakes and bogs occur at present (Palacios et al. 2016). Radiocarbon datings from the studied alpine paleoecological records indicate that wetlands formed in the area above ~2500 m after deglaciation (Fig. 2; Table 1). The different absolute ages for the beginning of sedimentation in different basins seems to be related to climate events and/or orientation of the studied sites (Manzano et al. 2019). Two south-facing sites, LdRS (3020 m) and LH (2899 m), accumulated sediments for the entire (or most of the) Holocene with estimated ages for the beginning of sedimentation of about 11,000 cal yr BP. Sediments in those two basins started accumulating right after deglaciation due to climate warming. Sediment

accumulation began somewhat later, at ~8200 cal yr BP, at two other sites located in the north face, BdlV (2945 m) and LdlMo (2889 m). Two alternative hypotheses should be considered to explain this. Firstly, it is possible that any sediments that accumulated during the Early Holocene in those basins were eroded by a short glaciation during the well-known 8.2 ka cold-arid event. However, there is no direct evidence of glaciation at that time in the Sierra Nevada (See Palacios et al. 2016). Secondly, coarse sands-conglomerates could have been deposited in the studied basins due to enhanced erosion caused by especially cold-dry conditions by the ~8200 cal yr BP event, and sediments below that coarse layer could not be retrieved by our coring methods. Two additional sediment records from LdlM (2497 m) and BdlC (2992 m), located in the north and south face, respectively, have basal sediment accumulation ages between ~4400 and 4100 cal yr BP. Interestingly, this coincides in time with the well-known 4.2 ka arid climatic event and the Middle-Late Holocene transition (Zielhofer et al. 2019). Perhaps, as mentioned above, older sediments were eroded from the basins due to particularly arid conditions at that time (see next section below) and/or our coring technique precluded us from recovering the older part of the sedimentary sequence from those two basins. The studied records show that sediment accumulation seems to be continuous after the formation of the wetlands in the alpine sedimentary basins (Fig. 2).

4.2 Changes in Lithology and MS in Relation with Climate and Human Impact

MS, a measure of the tendency of sediment to carry a magnetic charge (Snowball and Sandgren 2001), is in alpine lakes mostly related to the relative abundance of detritics (thus magnetic minerals) and organic matter in the sediments. MS is relatively lower when organic matter is abundant, as it is a diamagnetic material (Dearing 1999).

MS maxima during the Early Holocene could be related with maxima in winter precipitation and thus maxima in snowpack and highest summer insolation, melting the snow and producing a large amount runoff, fluvial erosion and sedimentation of detritics into the alpine sedimentary basins. Highest summer insolation at this time generated highest evaporation in summer at lower elevations and low lake level in Padul, with the development of marshy vegetation and sedimentation of peat, depicting low MS in this record (Ramos-Román et al. 2018b; Camuera et al. 2018),

Middle Holocene is characterized by minima in MS in the alpine sedimentary basins, warm but decreasing summer insolation and still quite humid conditions most likely benefited vegetation and algae to flourish in the Sierra Nevada environments, generating a major content in organics in the sediments deposited in the basins with respect to detritics. Decreasing precipitation, particularly in winter snowpack, at this time (Ramos-Román et al. 2018b) might have also produced a reduction in erosion and sedimentation in the studied Sierra Nevada basins. Perhaps both factors were in play at that time.

MS shows an overall increasing trend in the Late Holocene. This increase in MS has previously been interpreted as produced by enhanced erosion and increase in siliciclastic sediments due to a decrease in winter precipitation, enhanced aridification and decrease in forested vegetation in the area related to a decrease in summer insolation (Jiménez-Moreno and Anderson 2012; Fletcher et al. 2013). The occurrence of small glaciers in the highest catchment areas during several phases of the Late Holocene at ~2800–2700, 1400–1200 cal yr BP and during the Little Ice Age (1300–1850 CE) could have also generated enhanced erosion in the study area (Oliva et al. 2020). Finally, a clear increase in land use is also observed during the last ~1550 cal yr BP in Padul (Ramos-Román et al. 2018a), suggesting that humans could have been partially responsible for this sedimentary change.

4.3 Inorganic Geochemistry—Holocene Evolution of Lake-Level Changes, Runoff and Dust Deposition in Relation with Climate Change and Human Impact

Inorganic geochemistry data from the Sierra Nevada wetland sedimentary records inform us about variations in the lithology related to changes in the local depositional environment as well as with allochthonous sediment inputs into the basins (e.g., aeolian dust deposition) (Jiménez-Espejo et al. 2014; García-Alix et al. 2018). The rocks that occur in the Sierra Nevada alpine wetland drainage basins are metamorphic mica schists (rich in mica and feldspars with abundant Si, K, Al) (Camuera et al. 2018). Therefore, the K/Al and K/Ti ratios can be interpreted as detrital inputs, and thus a proxy of surface runoff. In this respect, the highest K/Ti ratio reached from ~11,000 until ~7000 cal yr BP in LH points to the wettest climate conditions recorded in the Sierra Nevada during the Early and Middle Holocene (Fig. 3). This, together with lowest values in Ca/Al, Ca/Ti and Zr/Al ratios also recorded in LH, suggests that runoff dominated over eolian inputs at that time (Mesa-Fernández et al. 2018; see explanation about eolian proxies below).

The inorganic geochemistry data show a trend toward more arid conditions in the Middle and Late Holocene in the Sierra Nevada. This is deduced by decreasing K/Ti ratios in LH in the last ~7000 cal yr BP (Mesa-Fernández et al. 2018; Fig. 3). Further support of enhanced aridity comes from the patterns observed in typical Saharan eolian dust input proxies, such as

the Zr/Th (Zr/Al, Ca/Ti, or Ca/Al) data from LdRS, LH and BdlC, which show minima in the Early and early-Middle Holocene and an increasing trend in the last ~7000 cal yr BP (Jiménez-Espejo et al. 2014; Mesa-Fernández et al. 2018; García-Alix et al. 2017). Zr/Th (Zr/Al) and Ca/Al (Ca/Ti) ratios have been used as eolian input proxies because Saharan dust is enriched in heavy minerals such as zircons, rutiles, as well as carbonates, which are absent in the alpine Sierra Nevada drainage basins (Mesa-Fernández et al. 2018). These ratios have been extensively used as a proxy of aeolian input in the Mediterranean or Atlantic regions (e.g., Rodrigo-Gámiz et al. 2011; Martínez-Ruiz et al. 2015). Enhanced eolian dust emissions from the Sahara were probably due to a coetaneous loss of vegetation cover in North Africa (Jiménez-Espejo et al. 2014).

Anthropogenic heavy metal atmospheric pollution at these high elevation Sierra Nevada wetlands was tracked using the Pb and Pb/Al data from selected sedimentary records (García-Alix et al. 2013; Mesa-Fernández et al. 2018). Pb/Al data from LdRS and LH show low values during most of the Holocene but increased in the Late Holocene, with peaks around 3000–2500, 2000 cal yr BP and between 1950–1970 AD (García-Alix et al. 2013; Mesa-Fernández et al. 2018). Lead was intensively extracted during the Late Bronze and Early Iron ages (~3500–2500 cal yr BP/~1550–550 cal BC) for metallurgical activities. It was used for ternary alloys (lead, tin and copper) and in cupellation processes. The development of cupellation processes in the southwestern Iberia pyritic belt for silver extraction led to an intensive exploitation of southeastern Iberia lead outcrops. High lead pollution is observed during the Roman Empire (between ~2100 and ~1700 cal yr BP), which is coherent with other regional records and data from historical sources (García-Alix et al. 2013). Maximum values of lead pollution in the Sierra Nevada are recorded in the last decades, between the 1950–1970 AD, related to the use of leaded-fuel in vehicles (García-Alix et al. 2013). Subsequently, the increase in unleaded-fuels, and the environmental alertness about lead emissions generated a decrease in lead pollution, which is clearly documented with a reduction in Pb/Al in the Sierra Nevada records (García-Alix et al. 2013; Mesa-Fernández et al. 2018; Fig. 3).

4.4 Organic Geochemistry—Total Organic Carbon Content and C/N Ratio in Relation with Climate, Temperature Estimations and Precipitation Patterns Derived by Specific Organic Lipids

Organic geochemistry data from bulk sediments such as total organic carbon (TOC) content, carbon to nitrogen atomic ratio (C/N), and stable carbon isotopes ($\delta^{13}C$), together with specific lipid biomarkers (*n*-alkanes: P_{aq}, long chain diols: LDI), give us insight about the biological sources of the organic matter and past biogeochemical cycles in the Sierra Nevada wetlands.

The C/N ratio can be used as a proxy for organic matter source in lacustrine sediments (Meyers 1994; Meyers and Teranes 2001). Protein-rich and cellulose-poor organic matter from lake algae is generally characterized by C/N values around 10, whereas values for protein-poor and cellulose-rich vascular land plants regularly exceed 20. A mix of algal and vascular plant organic matter is thus depicted by intermediate values (Meyers 1994; Meyers and Teranes 2001). $\delta^{13}C$ data from bulk sediments can be used to identify sources of organic matter and productivity levels (Talbot 2001). C3 vascular plants and lake algae are characterized by a similar $\delta^{13}C$ under normal conditions (Meyers 1994; Meyers and Teranes 2001). However, $\delta^{13}C$ increase in vascular plants during dry conditions and thus can be read in terms of water use efficiency (Farquhar et al. 1982). Algae preferentially incorporate the lighter C isotopes from the water's dissolved inorganic carbon pool. As a consequence, an algae productivity bloom enriches the carbon isotopic composition of the water, leading to the same isotopic enrichment in the algae from water mass (O'Leary 1988; Wolfe et al. 2001). Low C/N values in the Sierra Nevada records during the Early and Early-Middle Holocene suggested that the source of organic matter was mixed aquatic (algal)/terrestrial and very influenced by algae (Jiménez-Espejo et al. 2014; García-Alix et al. 2017). This points to relatively high lake levels in the LdRS and BdlV wetlands, which agrees with high humid climate conditions interpreted for this time period (Jiménez-Espejo et al. 2014; García-Alix et al. 2017). The highest $\delta^{13}C$ reached during this time interval in BdlV also implies significant algal productivity (García-Alix et al. 2012; Fig. 5). A major shift in the environment between 6000 and 5000 cal yr BP is observed through the significant increase in the C/N records from the Sierra Nevada. In LdRS this increase was interpreted as enhanced sedimentation of terrestrial vegetation with respect to algae related to a lowering of lake level and decrease in lake productivity. In BdlV, this increasing pattern was interpreted as a transition from a lake to a bog in the Middle Holocene, which also agrees with the $\delta^{13}C$ data and pollen and algae records (García-Alix et al. 2017; Fig. 5). Less precipitation and high evaporation rates may have caused the transition from a small lake to a bog in BdlV. Other alpine bogs such as BdlC also developed in the Sierra Nevada during the Middle Holocene at ~4400 cal yr BP. This agrees with the decrease in precipitation deduced by the decrease in arboreal pollen at this time (Fig. 6). C/N > 20 and $\delta^{13}C$ data from BdlV indicate that biomass production was dominated mainly by vascular terrestrial plants between ~5000 and ~4000 cal yr BP. From 4000 cal yr BP on,

C/N values decreased in all the studied records from the Sierra Nevada indicating more aquatic primary production in lakes and the development of occasional aquatic environments in peatlands. In the last 300 cal yr BP, the BdlC and BdlV records show a rapid and significant increase. C/N records in BdlC, LdM and LdRS registered a significant decrease in C/N in the last decades; however, the BdlV record did not register a substantial drop, suggesting that wetlands can display different responses to climate within the same Sierra Nevada region, depending on the landscape and the environmental evolution of the area. In any case, the abrupt environmental responses shown by the C/N records pointed to an amplification of natural trends caused by human pressure (García-Alix et al. 2017; see chapter "Paleolimnological Indicators of Global Change").

TOC content in the bulk sediment records gives insight about how much organic material occurs in the sediments with respect to the detrital fraction, and thus wetland productivity. In addition, the *n*-alkane abundance and distribution has been used as indicators of biological sources of organic matter accumulated in sediment records (e.g., Ficken et al. 2000; Eglinton and Eglinton 2008). *N*-alkanes derived from leaf plant waxes are proven to be extremely resistant to degradation during the transport and to the diagenesis, allowing its study lake records and providing information about vegetation and hydrological changes (e.g., Eglinton and Eglinton 2008). In general, *n*-alkanes with 21, 23 and 25 carbon atoms are associated with submerged and floating aquatic plants, expressed as P_{aq} (Cranwell 1984; Ficken et al. 2000). TOC and P_{aq} (deduced from leaf waxes, *n*-alkanes) values in LdRS are consistent with precipitation changes inferred from the local Sierra Nevada pollen and inorganic geochemistry records throughout the Holocene (Figs. 4, 5 and 6). Maxima in TOC and P_{aq} were reached during the Early and early-Middle Holocene, indicating maxima in algal productivity and deepest lake levels, and since ~6000 cal yr BP values have decreased until present. This was interpreted as related to the climate aridification process previously described in the Middle and Late Holocene (Jiménez-Espejo et al. 2014; Toney et al. 2020).

The fractional abundance of some long chain diols ($C_{28\text{-}30}$ 1,13- and 1,15-diols) expressed in the Long chain diol Index (LDI) is proven to be related to the superficial temperature of the water in which the algal sources grew (Rampen et al. 2014). The LDI has been successfully applied in the LdRS in the Sierra Nevada (Fig. 5) (García-Alix et al. 2020; Toney et al. 2020). The very good correlation between mean annual air temperature (MAAT) data of the last ~100 years and the LdRS LDI record permitted the utilization of this index as paleotemperature proxy for the Sierra Nevada (García-Alix et al. 2020). The LDI-inferred temperatures show that MAAT fluctuated around ~2.4 °C during the Holocene. MAAT changed around this mean value during the Early-Middle Holocene but changes occurred during the Middle to Late Holocene transition. Reconstructed temperatures reached a peak between ~5000 and 4200 cal yr BP, recording positive MAAT Anomalies (MAATAs). The especially warm period of the Middle Holocene ended abruptly at around 4150–4100 cal yr BP, reaching a minimum MAAT of −1.5 °C at ~4000 cal yr BP. Reconstructed Late Holocene temperatures oscillated around the average MAATA until ~1020 cal yr BP, when MAATA increased significantly to −0.5 °C during the well-known warm period of the Medieval Climate Anomaly (MCA; Moreno et al. 2012). Later on, temperatures decreased during the Little Ice Age (LIA), reaching the lowest value of the record at ~260 cal yr BP (−2.2 °C MAATA). Estimated temperatures increased later on until present, except for a sharp and short decline at the beginning of the twentieth century (−1.7 °C MAATA). Increasing temperature trends during the twentieth century match the temperature changes measured during the current global warming (García-Alix et al. 2020; IPCC 2013).

4.5 Palynological Analysis—Holocene Forest, Landscape and Lake Level Variations Due to Climate Change and Human Impact

Variations in the abundance of arboreal pollen (AP, including Mediterranean tree species) have previously been used in the Sierra Nevada records as a proxy for regional climate changes (Jiménez-Moreno and Anderson 2012; Ramos-Román et al. 2016, 2018a, b; Camuera et al. 2019). Increases in AP in the alpine records indicate enhanced humidity (overall, trees require more soil humidity than most herbs/shrubs) and proximity of forest (i.e., treeline) to the alpine wetlands, thus indicating increases in temperature as treeline moves to higher elevation during climate warming (Camuera et al. 2019).

A transition period from glacial to interglacial climate conditions occurred in the Sierra Nevada area during the earliest Holocene (~11,700 to 10,000 cal yr BP). This is shown in the oldest part of the sedimentary record of LdRS, which indicates steppe-like vegetation (*Artemisia*, Amaranthaceae, *Ephedra*), pointing to very arid and cold conditions. Regionally, similar pollen data have been recorded in Carihuela Cave (Fernández et al. 2007; Carrión et al. 2019), as well as in marine records from the Alboran Sea (Dormoy et al. 2009; Fletcher et al. 2010). In the lower-elevation Padul area, this transition seems to have occurred faster (from 11,700 to 11,000 cal yr BP) and was characterized by pollen assemblages dominated by evergreen *Quercus* and to a lesser extent deciduous *Quercus*. The increase in Mediterranean forest species recorded in the Sierra Nevada pollen records could be interpreted as a regional vegetation

response to warmer and more humid climate conditions, generating a displacement of forest species toward higher elevations and more heavily tree-populated forest.

Palynological records indicate that a maximum in temperature and humidity occurred in the Sierra Nevada area between ~10,500 and 7000 cal yr BP (Fig. 6). This is indicated by the highest abundance of tree species and the abundance of algae (*Botryococcus* and *Pediastrum*) in the studied records. The abundance of high-elevation *Pinus* species indicates that the highest elevation of treeline was reached in the Sierra Nevada subalpine area at this time. In the Padul-15–05 record the highest values of Mediterranean forest also occurred at that time, showing an expansion in mesic forest species (e.g., deciduous *Quercus*). Both regional (Burjachs et al. 1997; Fletcher and Sánchez Goñi 2008) and global studies show a humid and warm Early Holocene (Jalut et al. 2009; Brayshaw et al. 2011). A very warm Early Holocene could be explained by maximum summer insolation at this time that would have produced climate warming. The maximum humidity between ~10,500 and 7000 cal yr BP could be explained by an increase in the land/sea temperature contrast in the Mediterranean region during autumn, which would favor an increase in rainfall during autumn/winter seasons (Tuenter et al. 2003; Meijer and Tuenter 2007).

The Sierra Nevada pollen records show a progressive process of forest reduction, increase in xerophytes (i.e., *Artemisia*, Amaranthaceae or Caryophyllaceae), and decrease in aquatic species in the wetlands in the Middle and Late Holocene (Fig. 6). This trend, which begins after ~7000 cal yr BP and intensifies after ~6000–5000 cal yr BP, could be explained by a progressive climatic cooling and, mostly, by an increase in aridity. This aridification process has been observed in other pollen records in this region (e.g., Sierra de Cazorla: Carrión 2002; Alboran Sea: Fletcher et al. 2010; SW Iberian Peninsula: Jiménez-Moreno et al. 2015) and from many other paleoclimatic indicators for the entire Mediterranean region (speleothems, lake levels, river and wind inputs; Jalut et al. 2009). This climate change, decrease in temperature and increase in aridity, is explained by the decrease in summer insolation (Cacho et al. 2002; Renssen et al. 2003). Another evidence of aridification in the Sierra Nevada during the Middle and Late Holocene is the interpretation of decreasing lake levels in some of the longest studied alpine records (Anderson et al. 2011; Jiménez-Moreno and Anderson 2012). This was interpreted after noticing a considerable decline in aquatic algae species.

4.5.1 Millennial-Scale Climate Variability

Sierra Nevada pollen records show shorter-scale cyclical changes superimposed on the main climate trend toward increased aridity. Significant forest declines occurred around 7500, 6500, 5000 and 4200, 3000 and 1200 cal yr BP (Fig. 6). Some of these forest declines can be interpreted as generated by severe and persistent drought conditions, which have been recognized regionally and globally at those times (see summary in Jiménez-Moreno and Anderson, 2012; Ramos-Román et al. 2018b). For example, the drought that characterized the MCA (Moreno et al. 2012) is very well documented in the LdlM record (Jiménez-Moreno et al. 2013). Among arid periods there were others that were relatively more humid, translated into enhanced forest development such as that observed in LdlM, BdlC, LH or Padul, coinciding with the maximum humidity of the Iberian Roman Humid Period (IRHP) or the LIA (Jiménez-Moreno et al. 2013; Ramos-Román et al. 2016, 2018a; Mesa-Fernández et al. 2018). These climatic variations were probably related with large-scale cyclical changes in the frequency of the North Atlantic Oscillation (NAO) atmospheric phenomenon and arid periods were due to persistent phases of NAO+ and more humid periods to persistent phases of NAO-. For example, wetter climatic conditions during the LIA period were probably related to persistent NAO- conditions, which at present-day produces a general increase in winter precipitation in the area (Trouet et al. 2009; Mesa-Fernández et al. 2018; Ramos-Román et al. 2016, 2018a; Jiménez-Moreno et al. 2020).

4.5.2 Human Impact on Vegetation, Grazing and Cultivation

In the last millennia human impact on the Sierra Nevada vegetation has increased and changes in the vegetation are more difficult to interpret. Climate has been a major driver of vegetation change in this area but human impact cannot be neglected (Anderson et al. 2011; Jiménez-Moreno and Anderson 2012, 2018a; Manzano et al. 2019). Pollen data show that since 3000 cal yr BP humans had an impact in Sierra Nevada with evidence of grazing and cultivation (Anderson et al. 2011; Jiménez-Moreno and Anderson, 2012). However, the anthropogenic impact was relatively small until ~1500 cal yr BP and intensified in the last ~500 years with large-scale olive cultivation at lower altitudes and pine reforestation in the last century (Ramos-Román et al. 2019).

Early evidences of grazing in alpine Sierra Nevada come from the *Sporormiella* spore records. *Sporormiella* is a genus of coprophilous fungi that requires herbivore digestion to complete its life cycle, producing spores in the excrements (Anderson et al. 2011). Their increasing abundance in the last 2700 cal yr BP, becoming very abundant in the last millennium (Anderson et al. 2011; Jiménez-Moreno and Anderson 2012; Ramos-Román et al. 2018a; Manzano et al. 2019) probably indicates intensified grazing in the higher elevations of the Sierra Nevada at this time related with the introduction of livestock on the landscape. Enhanced grazing roughly concurs with the first signs of

cultivation with occurrences of Cerealia (cereal grass) pollen, most likely planted at lower elevations (Jiménez-Moreno and Anderson 2012; Manzano et al. 2019), and land-use indicators such as *Rumex*, *Plantago*, *Urtica*, Convolvulaceae or Asteraceae, which are consistent in the pollen records since the last 3000–2000 cal yr BP, and enhanced in the last ~1500 cal yr BP (Ramos-Román et al. 2018a).

Olea cultivation boosted in the last 1000 years in the Sierra Nevada area (Ramos-Román et al. 2019). A further increasing trend in *Olea* cultivation happened in the last 150 cal yr BP, during the industrial revolution, which was probably triggered by improvements in agricultural practices. A more recent widespread cultivation and olive oil production increase occurred in Spain in the mid-twentieth century (Ramos-Román et al. 2019). Finally, the twentieth century *Pinus* pollen increase (reflected in the AP; Fig. 6) reproduces the extensive human-induced reforestation with pines, done for forest restoration and to prevent soil erosion previously generated by natural and anthropogenic deforestation.

In summary, pollen data from the Sierra Nevada show that human impact on the Sierra Nevada environments was insignificant until the last ~1500 cal yr BP and was less pronounced than in other lower elevation regions of southern Iberia (Anderson et al. 2011).

4.6 Charcoal Analysis—Fire Activity Related to Climate and Fuel Variability

Charcoal analysis is based on the accumulation of charcoal particles in sedimentary records during and after a fire event. Sedimentary layers with abundant charcoal are inferred to result from past fire activity (Whitlock and Anderson 2003). Macroscopic charcoal particles (>100 μm) indicate occurrence of nearby fires, because particles of this size do not travel far from their source (Whitlock and Anderson 2003). The charcoal analysis on the Sierra Nevada sedimentary records, combined with palynological and geochemical proxies, permit us to study how fire regimes were affected by periods of major climate change and vegetation reorganization in the past.

Charcoal particles were generally not abundant in the alpine Sierra Nevada records (Fig. 7). This can be explained by a faraway origin of charcoal particles, probably from fires that occurred at lower elevations in this mountain range, as natural fires are extremely rare above treeline in the Sierra Nevada at present and were probably very rare in the past. Considering this relationship, these charcoal records show that fire activity was relatively high during the Middle Holocene between ~7500 and 6700 cal yr BP, decreasing later on. The decrease in fire activity at ~7000 cal yr BP could have been conditioned by a decrease in forest fuel due to the progressive loss in Mediterranean forest previously discussed and due to enhanced aridification (Fig. 6). However, enhanced fire activity in this region is observed since ~3000 cal yr BP (Fig. 7; Anderson et al. 2011; Jiménez-Moreno et al. 2013; Ramos-Román et al. 2016) and maxima in charcoal concentration occurred between ~2700 to 1600 cal yr BP in LdlM, BdlC and LdRS records, coinciding with the time of the IRHP (2600–1600 cal yr BP, Martín-Puertas et al. 2009), the most humid period detected in the area during the Late Holocene in the Sierra Nevada. Many charcoal records from the western Mediterranean region show maxima in fire activity around that time. For example, the nearby Sierra de Baza record depicts remarkable similarities to the Sierra Nevada records with charcoal maxima at ~2000 cal yr BP (Carrión et al. 2007), but also charcoal maxima around that time was observed in the Sierra de Gádor (Carrión et al. 2003), Alboran Sea (Combourieu Nebout et al. 2009) and Djamila, in northern Morocco (Linstädter and Zielhofer 2010). This regional agreement about enhanced fire activity between 3000 and 2000 cal yr BP may have been related to increased forest, and therefore fuel loads on the landscape due to enhanced humidity. This supports the hypothesis of Mediterranean fire regimes today being controlled by fuel load variations (Daniau et al. 2007; Linstädter and Zielhofer 2010). Charcoal decreased considerably after this IRHP peak, during the Dark Ages (DA) and MCA, when warmer and drier conditions occurred (Moreno et al. 2012; García-Alix et al. 2020; Fig. 7). This was probably due to the decrease in forest fuel, which agrees with the decline in forest species recorded in the Sierra Nevada at that time (Fig. 6; Jiménez-Moreno et al. 2013; Ramos-Román et al. 2016, 2018a; Mesa-Fernández et al. 2018).

Even though we believe that patterns recorded in the charcoal records from the Sierra Nevada mostly responded to natural climate variability, the increase in charcoal in the last millennia could have also been due to increased human activity (i.e., forest burning) due to accelerated mining, cultivation and grazing activities (Anderson et al. 2011; García-Alix et al. 2013; see also discussion above).

5 Conclusions

Multi-proxy sedimentary records from the Sierra Nevada wetlands show the warmest and wettest climate conditions during the Early and early-Middle Holocene (from ~11,000 to 7000 cal yr BP), related to Holocene summer insolation maxima. Such optimum climate conditions translated into high detrital sedimentation, maximum Mediterranean forest expansion in density and elevation in the Sierra Nevada, and the highest lake levels in the alpine area.

Multiple evidences show a long-term aridification of the Sierra Nevada environment since ca. 7000 cal yr BP until

today, probably related to a decrease in precipitation generated by a decrease in summer insolation during the Middle and Late Holocene. This is mostly deduced by a decrease in runoff, a decrease in forest species, particularly in *Pinus* and *Quercus* and other mesophyte species and lower lake levels in alpine environments. This agrees with enhanced Saharan eolian dust input in the alpine records.

This long-term aridification trend was interrupted by short time-scale millennial-scale variability evident in our records by decreases in forest that could be related to arid and/or cold events at ~7500, 6500, 5200, 4200, 3000 and 1200 cal yr BP. Some of these events, such as the one that affected the area during the MCA, coincide in the timing with droughts that affected the wider Mediterranean area and other distant regions, and could be related to persistent NAO + conditions in the study area.

In addition, humans also influenced environments in the Sierra Nevada in the last millennia. Charcoal increase, lead pollution and cultivar proxies indicate anthropogenic impact since 3000 cal yr BP. Human impact is particularly important in the last 1500 cal yr BP, with a strong increase in the palynological record of cultivars and grazing, significantly stronger in the last millennium with records of massive cultivation of *Olea* at lower elevations and *Pinus* reforestation. Estimated temperatures using the algal-derived lipids in the Sierra Nevada show a very high rate of warming in the last century and that human-derived greenhouse gases seem to be the major temperature driver in these high-elevation sites at present.

Sedimentary archives from the Sierra Nevada wetlands show a fast and very sensitive response of mountain ecosystems to climate change and human impact throughout the Holocene, reflecting climate events on a regional and global scale. Sierra Nevada is, therefore, especially sensitive to global change and important changes will occur in these alpine ecosystems (e.g., eutrophication, aridification, increase in fires) if the current temperature increase is not slowed or reversed. This study shows the importance of past and present monitoring of wetlands in mountain areas for a better understanding of climate variability and future rapid environmental responses.

Acknowledgements This study was supported by projects CGL2013-47038-R and CGL2017-85415-R funded by Ministerio de Economía y Competitividad of Spain and Fondo Europeo de Desarrollo Regional FEDER; Séneca Project 20788/PI/18; Junta de Andalucía I+D +i Junta de Andalucía 2020 Retos P-20-00059, FEDER Project B-RNM-144-UGR18, UGR-FEDER B-RNM-144-UGR18 Proyectos I + D + i del Programa Operativo FEDER 2018 and the research group RNM-190 (Junta de Andalucía). M.J.R.R. acknowledges the postdoctoral funding provided by the European Commission/H2020 (ERC-2017-ADG, project number 788616). J.C. acknowledges the postdoctoral funding provided by the Academy of Finland (project number 316702). A.G.-A. acknowledges the Ramón y Cajal fellowship RYC-2015-18966 provided by the Ministerio de Economía y Competitividad of the Spanish Government. M.R.G. acknowledges funding by the Juan de la Cierva-Incorporación program in the University of Granada (IJCI-2017-33755) from Secretaría de Estado de I+D+i, Spain. RSA acknowledges several travel grants from Northern Arizona University to support this work.

References

Anderson RS, Jiménez-Moreno G, Carrión JS, Pérez-Martínez C (2011) Holocene vegetation history from Laguna de Río Seco, Sierra Nevada, southern Spain. Quat Sci Rev 30:1615–1629

Beug H-J (2004) Leitfaden der Pollenbestimmung für Mitteleuropa und angrenzende Gebiete, Fisch. Stuttg., Leitfaden der Pollenbestimmung für Mitteleuropa und angrenzende Gebiete, Friedrich Pfeil, München

Blaauw M (2010) Methods and code for 'classical' age-modelling of radiocarbon sequences. Quat Geochron 5:512–518

Cacho I, Grimalt JO, Canals M (2002) Response of the Western Mediterranean Sea to rapid climatic variability during the last 50,000 years: a molecular biomarker approach. J Mar Sys 33–34:253–272

Cranwell PA (1984) Lipid geochemistry of sediments from Upton broad, a small productive lake. Org Geochem 7:25–37

Brayshaw DJ, Rambeau CMC, Smith SJ (2011) Changes in Mediterranean climate during the Holocene: insights from global and regional climate modelling. Holocene 21:15–31

Burjachs F, Giralt S, Roca JR et al (1997) Palinología holocénica y desertización en el Mediterráneo occidental. In: Ibáñez JJ, Valero BL, Machado C (eds) El paisaje mediterráneo a través del espacio y del tiempo. Implicaciones en la desertificación, Geoforma Editores, Logroño, pp 379–394

Camuera J, Jiménez-Moreno G, Ramos-Román MJ et al (2018) Orbital-scale environmental and climatic changes recorded in a new ~ 200,000-year-long multiproxy sedimentary record from Padul, southern Iberian Peninsula. Quat Sci Rev 198:91–114

Camuera J, Jiménez-Moreno G, Ramos-Román MJ et al (2019) Vegetation and climate changes during the last two glacial-interglacial cycles in the western Mediterranean: A new long pollen record from Padul (southern Iberian Peninsula). Quat Sci Rev 205:86–105

Camuera J, Jiménez-Moreno G, Ramos-Román MJ et al (2021) Chronological control and centennial-scale climatic subdivisions of the Last Glacial Termination in the western Mediterranean region. Quat Sci Rev 255:106814

Carrión JS (2002) Patterns and processes of Late Quaternary environmental change in a montane region of southwestern Europe. Quat Sci Rev 21:2047–2066

Carrión JS, Sánchez-Gómez P, Mota JF et al (2003) Fire and grazing are contigent on the Holocene vegetation dynamics of Sierra de Gádor, southern Spain. Holocene 13:839–849

Carrión JS, Fernández S, Jiménez J et al (2019) The sequence at Carihuela Cave and its potential for research into Neanderthal ecology and the Mousterian in southern Spain. Quat Sci Rev 217:194–216

Carrión JS, Fuentes N, González-Sampériz P (2007) Holocene environmental change in a montane region of sourthern Europe with a long history of human settlement. Quat Sci Rev 26:1455–1475

Combourieu Nebout N, Peyron O, Dormoy I et al (2009) Rapid climatic variability in the west Mediterranean during the last 25000 years from high resolution pollen data. Clim past 5:503–521

Daniau AL, Sánchez-Goñi MF, Beaufort L et al (2007) Dansgaard-Oeschger climatic variability revealed by fire emissions in southwestern Iberia. Quat Sci Rev 26:1369–1383

Dearing J (1999) Magnetic susceptibility. In: Walden J, Oldfield F, Smith J (eds) Environmental magnetism: a practical guide. Quaternary Research Association, London, pp 35–62

Dormoy I, Peyron O, Combourieu Nebout N et al (2009) Terrestrial climate variability and seasonality changes in the Mediterranean region between 15 000 and 4000 years BP deduced from marine pollen records. Clim past 5:615–632

Eglinton TI, Eglinton G (2008) Molecular proxies for paleoclimatology. Earth Planet Sci Lett 275:1–16

Faegri K, Iversen J (1989) Textbook of Pollen analysis. Caldwell. Blackburn Press, New Jersey, pp 69–90

Farquhar GD, O'Leary MH, Berry JA (1982) On the relationship between carbon isotope discrimination and the intercellular carbon dioxide concentration in leaves. Aust J Plant Physiol 9:121–137

Fernández S, Fuentes N, Carrión JS et al (2007) The Holocene and upper Pleistocene pollen sequence of Carihuela cave, southern Spain. Geobios 40:75–90

Ficken KJ, Li B, Swain D, Eglinton G (2000) An n-alkane proxy for the sedimentary input of submerged/floating freshwater aquatic macrophytes. Org Geochem 31:745–749

Fletcher WJ, Sanchez Goñi MF (2008) Orbital- and sub-orbital-scale climate impacts on vegetation of the western Mediterranean basin over the last 48,000 yr. Quat Res 70:451–464

Fletcher WJ, Sanchez Goñi MF, Peyron O, Dormoy I (2010) Abrupt climate changes of the last deglaciation detected in a Western Mediterranean forest record. Clim past 6:245–264

Fletcher WJ, Debret M, Sanchez Goñi MF (2013) Mid-Holocene emergence of a low frequency millennial oscillation in western Mediterranean climate: implications for past dynamics of the North Atlantic atmospheric westerlies. Holocene 23(2):153–166

García-Alix A, Jiménez-Moreno G, Anderson RS et al (2012) Holocene paleoenvironmental evolution of a high-elevation wetland in Sierra Nevada, southern Spain, deduced from an isotopic record. J Paleolimnol 48:471–484

García-Alix A, Jimenez-Espejo FJ, Lozano JA et al (2013) Anthropogenic impact and lead pollution throughout the Holocene in southern Iberia. Sci Total Environ 449:451–460

García-Alix A, Jiménez-Espejo FJ, Toney JL et al (2017) Alpine bogs of southern Spain show human-induced environmental change superimposed on long-term natural variations. Sci Rep 7:7439

García-Alix A, Jiménez-Espejo FJ, Jiménez-Moreno G et al (2018) Holocene geochemical footprint from Semi-arid alpine wetlands in southern Spain. Sci Data 5:180024

García-Alix A, Toney JL, Jiménez-Moreno G et al (2020) Algal lipids reveal unprecedent warming rates in alpine areas of SW Europe during the Industrial Period. Clim past 16:245–263

Gehrig-Fasel J, Guisan A, Zimmermann NE (2008) Evaluating thermal treeline indicators based on air and soil temperature using an air-to-soil temperature transfer model. Ecol Model 213:345–355

Heegaard E, Birks HJB, Telford RJ (2005) Relationships between calibrated ages and depth in stratigraphical sequences: an estimation procedure by mixed-effect regression. Holocene 15:612–618

IPCC (2013) Climate change 2013: the physical science basis. In: Contribution of working group I to the fifth assessment report of the Intergovernmental Panel on Climate Change. Cambridge University Press, Cambridge, United Kingdom and New York, USA

Jalut G, Dedoubat JJ, Fontugne M, Otto T (2009) Holocene circum-Mediterranean vegetation changes: climate forcing and human impact. Quat Inter 200:4–18

Jiménez-Espejo FJ, García-Alix A, Jiménez-Moreno G et al (2014) Saharan aeolian input and effective humidity variations over Western Europe during the Holocene. Chem Geol 374–375:1–12

Jiménez-Moreno G, Anderson RS (2012) Holocene vegetation and climate change recorded in alpine bog sediments from the Borreguiles de la Virgen, Sierra Nevada, southern Spain. Quat Res 77:44–53

Jiménez-Moreno G, García-Alix A, Hernández-Corbalán MD et al (2013) Vegetation, fire, climate and human disturbance history in the southwestern Mediterranean area during the late Holocene. Quat Res 79:110–122

Jiménez-Moreno G, Rodríguez-Ramírez A, Pérez-Asensio JN et al (2015) Impact of late-Holocene aridification trend, climate variability and geodynamic control on the environment from a coastal area in SW Spain. Holocene 25:607–617

Jiménez-Moreno G, Anderson RS, Ramos-Román MJ et al (2020) The Holocene Cedrus pollen record from Sierra Nevada (S Spain), a proxy for climate change in N Africa. Quat Sci Rev 242:106468

Laskar J, Robutel P, Joutel F, Gastineau M, Correia ACM, Levrard B (2004) A long term numerical solution for the insolation quantities of the Earth. Astron. Astrophys. Nor 428:261–285

Linstädter A, Zielhofer C (2010) Regional fire history shows abrupt responses of Mediterranean ecosystems to centennial-scale climate change (Olea–Pistacia woodlands), NE Morocco. J Arid Environ 74:101–110

Löwemark L, Chen H-F, Yang T-N et al (2011) Normalizing XRF-scanner data: a cautionary note on the interpretation of high-resolution records from organic-rich lakes. J Asian Earth Sci 40:1250–1256

Malanson GP, Resler LM, Butler DR, Fagre DB (2019) Mountain plant communities: uncertain sentinels? Prog Phys Geogr 43:521–543

Manzano S, Carrión JS, López-Merino L et al (2019) A palaeoecological approach to understanding the past and present of Sierra Nevada, a Southwestern European biodiversity hotspot. Global Planet Change 175:238–250

Martín-Puertas C, Valero-Garcés BL, Brauer A et al (2009) The Iberian-Roman Humid Period (2600–1600 cal yr BP) in the Zoñar lake varve record (Andalucía, southern Spain). Quat Res 71:108–120

Martínez-Ruiz F, Kastner M, Gallego-Torres D et al (2015) Paleoclimate and paleoceanography over the past 20,000 yr in the Mediterranean Sea Basins as indicated by sediment elemental proxies. Quat Sci Rev 107:25–46

Mesa-Fernández JM, Jiménez-Moreno G, Rodrigo-Gámiz M et al (2018) Vegetation and geochemical response to Holocene rapid climate change in the Sierra Nevada (southeastern Iberia): the Laguna Hondera record. Clim past 14:1687–1706

Meijer PTh, Tuenter E (2007) The effect of precession-induced changes in the Mediterranean freshwater budget on circulation at shallow and intermediate depth. J Mar Sys 68:349–36

Meyers PA (1994) Preservation of elemental and isotopic source identification of sedimentary organic matter. Chem Geol 113:289–302

Meyers PA, Teranes JL (2001) Sediment organic matter. In: Last WM, Smol JP (eds) Tracking environmental changes using lake sediments, vol 2. Kluwer, Dordrecht, pp 239–270

Moreno A, Pérez A, Frigola J et al (2012) The Medieval Climate Anomaly in the Iberian Peninsula reconstructed from marine and lake records. Quat Sci Rev 42:16–32

O'Leary MH (1988) Carbon isotopes in photosynthesis. Bioscience 38:328–336

Oliva M, Gómez-Ortiz A, Palacios D et al (2020) Multiproxy reconstruction of Holocene glaciers in Sierra Nevada (south Spain). Med Geos Rev 2:5–19

Palacios D, Gómez-Ortiz A, Andrés N et al (2016) Timing and new geomorphologic evidence of the last deglaciation stages in Sierra Nevada (southern Spain). Quat Sci Rev 150:110–129

Páscoa P, Gouveia CM, Russo A, Trigo RM (2017) Drought trends in the Iberian Peninsula over the last 112 years. Adv Meteorol 2017:4653126

Pausas JG, Fernández-Muñoz S (2012) Fire regime changes in the western Mediterranean basin: from fuel limited to drought-driven fire regime. Clim Change 110:215–226

Ramos-Román MJ, Jiménez-Moreno G, Anderson RS (2016) Centennial-scale vegetation and North Atlantic Oscillation changes during the late Holocene in the western Mediterranean. Quat Sci Rev 143:84–95

Ramos-Román MJ, Jiménez-Moreno G, Camuera J et al (2018a) Holocene climate aridification trend and human impact interrupted by millennial and centennial-scale climate fluctuations from a new sedimentary record from Padul (Sierra Nevada, southern Iberian Peninsula). Clim past 14:117–137

Ramos-Román MJ, Jiménez-Moreno G, Camuera J (2018b) Millennial-scale cyclical environment and climate variability during the Holocene in the western Mediterranean region deduced from a new multiproxy analysis from the Padul record (Sierra Nevada, Spain). Global Planet Change 168:35–53

Ramos-Román MJ, Jiménez-Moreno G, Anderson RS et al (2019) Climate controlled historic olive tree occurrences and olive oil production in southern Spain. Global Planet Change 182:102996

Reille M (1992) Pollen et Spores d'Europe et Afrique du Nord. Laboratoire de Botanique Historique et Palynologie, Marseille

Reimer PJ, Bard E, Bayliss A et al (2013) IntCal13 and Marine13 radiocarbon age calibration curves 0–50,000 years cal BP. Radiocarbon 55:1869–1887

Renssen H, Brovkin V, Fichefet T, Goosse H (2003) Holocene climate instability during the termination of the African Humid Period. Geophys Res Lett 30:1184

Rodrigo-Gámiz M, Martínez-Ruiz F, Jiménez-Espejo FJ et al (2011) Impact of climate variability in the western Mediterranean during the last 20,000 years: oceanic and atmospheric responses. Quat Sci Rev 30:2018–2034

Snowball I, Sandgren P (2001) Application of mineral magnetic techniques to paleolimnology. In: Last WM, Smol JP (eds) Tracking environmental changes using lake sediments, vol 2. Kluwer Academic Publishers, Dordrecht, pp 217–237

Sousa PM, Trigo RM, Pereira MG et al (2015) Different approaches to model future burnt area in the Iberian Peninsula. Agric for Meteorol 202:11–25

Sousa PM, Barriopedro D, Ramos AM et al (2019) Saharan air intrusions as a relevant mechanism for Iberian heatwaves: the record breaking events of August 2018 and June 2019. Weather Clim Extr 26:100224

Talbot MR (2001) Nitrogen isotopes in palaeolimnology. In: Last WM, Smol JP (eds) Tracking environmental changes using lake sediments: physical and chemical techniques. Kluwer, Dordrecht, pp 401–439

Thuiller W, Lavorel S, Araujo MB et al (2005) Climate change threats to plant diversity in Europe. PNAS 102:8245–8250

Toney JL, García-Alix A, Jiménez-Moreno G et al (2020) New insights into Holocene hydrology and temperature from lipid biomarkers in western Mediterranean alpine wetlands. Quat Sci Rev 240:106395

Trouet V, Esper J, Graham NE et al (2009) Persistent positive north Atlantic oscillation mode dominated the Medieval climate anomaly. Science 324:78–80

Tuenter E, Weber SL, Hilgen FJ, Lourens LJ (2003) The response of the African summer monsoon to remote and local forcing due to precession and obliquity. Glob Planet Change 36:219–235

Webster CE (2018) Late-Pleistocene and Holocene record of fire at Padul peat bog (Granada, Spain). MS Dissertation, Northern Arizona University

Whitlock C, Anderson RS (2003) Fire history reconstructions based on sediment records from lakes and wetlands. In: Veblen TT, Baker WL, Montenegro G, Swetnam TW (eds) Fire and climatic change in temperate ecosystems of the Americas, vol 160. Springer, New York, pp 3–31

Wolfe BB, Edwards TWD, Beuning KRM, Elgood RJ (2001) Carbon and oxygen isotope analysis of lake sediment cellulose: methods and applications. In: Last WM, Smol JP (eds) Tracking environmental changes using lake sediments: physical and chemical techniques. Kluwer, Dordrecht, pp 373–400

Zielhofer C, Köhler A, Mischke S et al (2019) Western Mediterranean hydro-climatic consequences of Holocene ice-rafted debris (Bond) events. Clim past 15:463–475